Monolithic optical gates based on integration of evanescently-coupled uni-traveling-carrier photodiodes and electroabsorption modulators*

Zhang Yun-Xiao(张云霄)†, Liao Zai-Yi(廖栽宜), Zhao Ling-Juan(赵玲娟), Pan Jiao-Qing(潘教青), Zhu Hong-Liang(朱洪亮), and Wang Wei(王 圩)

Key Laboratory of Semiconductors Materials, Institute of Semiconductors, Chinese Academy of Sciences, Beijing 100083, *China*

(Received 11 December 2009; revised manuscript received 30 December 2009)

We report on chip-scale optical gates based on the integration of evanescent waveguide unitraveling-carrier photodiodes (EC-UTC-PDs) and intra-step quantum well electroabsorption modulators (IQW-EAMs) on n-InP substrates. These devices exhibit simultaneously 2.1 GHz and −16.2 dB RF-gain at 21 GHz with a 450 Ω thin-film resistor and a bypass capacitor integrated on a chip.

Keywords: electroabsorption modulator, intra-step quantum wells, uni-traveling-carrier RF-gain
PACC: 4280S, 4280K, 2940P

1. Introduction

The high-speed optical network is the backbone of the internet today. As the internet data bandwidth continues to climb, the optical devices used to manipulate these data should be improved. Current optical networks are, however, restricted by the bottle-neck of optical-electron-optical conversion (OEO) technology,[1] which requires propagating high-speed signals in the electronic domain and cascading separately packaged electronic and optoelectronic devices, resulting in an increase in cost, size, weight, power consumption and heat radiation. The ultra-fast optical switch will be a key device for the next generation of the optical network because of its flexible application in optical signal processing, such as demultiplexing (DEMUX), 2R regeneration (reshaping and re-amplification), wavelength conversion, and so on.[2−4] Recently, the integration of photodiode (PD) and electroabsorption modulator (EAM) has drawn lots of attention due to its application in optical signal processing.[5−8] Different from traditional OEO conversion technology, such a PD–EAM gate has a very high speed-operation capacity because of its short electronic interconnecting distance and exemption of electronic amplification. An NTT corporation group has reported on an optical gate made by integrating a surface-illuminated uni-traveling-carrier photodiode with a waveguide EAM which possesses a very short gate opening time of 2.3 ps and is applied to several ultrafast optical signal processings.[5] However, this needs a PD input pulse energy of 5 pJ/pulse which means a requirement for large optical power consumption. We have reported on an optical gate by integrating a surface normal PIN photodiodeintegrated with a waveguide electro-absorption modulator that has achieved a conversion of arbitrary wavelength over 20 nm at 2.5 Gbit/s.[9] However, the dc bias voltage of PD was fixed at 8 V, which means a large electrical power consumption. In addition, this surface PD–EAM is hard to test and package because its three optical ports are not in the same plane.[10]

In the present work, a PD–EAM optical gate is fabricated on an N-InP substrate with an evanescent waveguide uni-traveling-carrier photodiode (EC-UTCPD)[11,12] and an intra-step quantum well electroabsorption modulator (IQWEAM)[13,14] for the first time. By comparison with the previously reported optical gate, the fabrication process of this new optical gate is as simple as that of a single EAM except for an additional metal organic chemical vapour deposition (MOCVD) growth. The EC-UTCPD has

*Project supported by the National High Technology Research and Development of China (Grant Nos. 2006AA01Z256, 2007AA03Z419 and 2007AA03Z417), the State Key Development Program for Basic Research of China (Grant Nos. 2006CB604901and 2006CB604902), and the National Natural Science Foundation of China (Grant Nos. 90401025, 60736036, 60706009 and 60777021).

†Corresponding author. E-mail: zhangyx@semi.ac.cn

© 2010 Chinese Physical Society and IOP Publishing Ltd

achieved high responsivity, high bandwidth and good saturation current operation at lower bias voltages.[15] The 3 dB bandwidth of this novel optical gate is about 2.1GHz and its RF-gain is about −16.2 dB at 2.1 GHz with a 450 Ω thin-film resistor.

2. Structure design and fabrication

Figure 1(a) shows a chip photograph of a fabricated optical gate employing monolithic integration of an EC-UTCPD, an IQWEAM, a bias capacitor and a load resistor on an S-doped InP substrate. Its total dimensions are 600 μm×400 μm. The interconnections of EC-UTC-PD and IQW-EAM electrodes are designed as microstrip transmission lines and configured such that the optical and the electrical signals propagate in the same directions to take advantage of traveling wave effects. The speed limiting factors in a traveling-wave EC-UTC-PD/EAM optical gate include microwave loss and optical-electrical group velocity mismatch. The group velocity mismatch is not a main speed limiting factor because of a very short interaction length. However, there exists a higher microwave propagation loss because of a larger shunt current passing through the n-doped substrate and a larger reflection loss resulting from the larger on-chip Ta_2N thin-film resistor. Therefore, this optical gate should be treated as a lumped device with a large on-chip Ta_2N thin-film resistor and its simplified circuit diagram is shown in Fig. 1(b). The on-chip bias capacitor ($C_{\rm in}$ ∼pF) is used for biasing both the EAM and PD and simultaneously confining all high-speed electrical signals within this compact integrated optical gate. A large capacitor ($C_{\rm ex}$ ∼ 1000 pF) is added to the carrier passing through a wirebond to extend the low frequency response. The value of wirebond inductance ($L_{\rm wirebond}$) is very small and can be neglected. For this optical gate structure, the 3dB bandwidth with ignoring the effects of the EAM current source and any parastics, is approximately given by:[16]

$$f_{\rm 3dBe} = \sqrt{3}/2\pi R_{\rm L}(C_{\rm PD} + C_{\rm EAM}), \qquad (1)$$

where $C_{\rm PD}$ and $C_{\rm EAM}$ are junction capacitances of PD and EAM respectively, and $R_{\rm L}$ is load resistor.

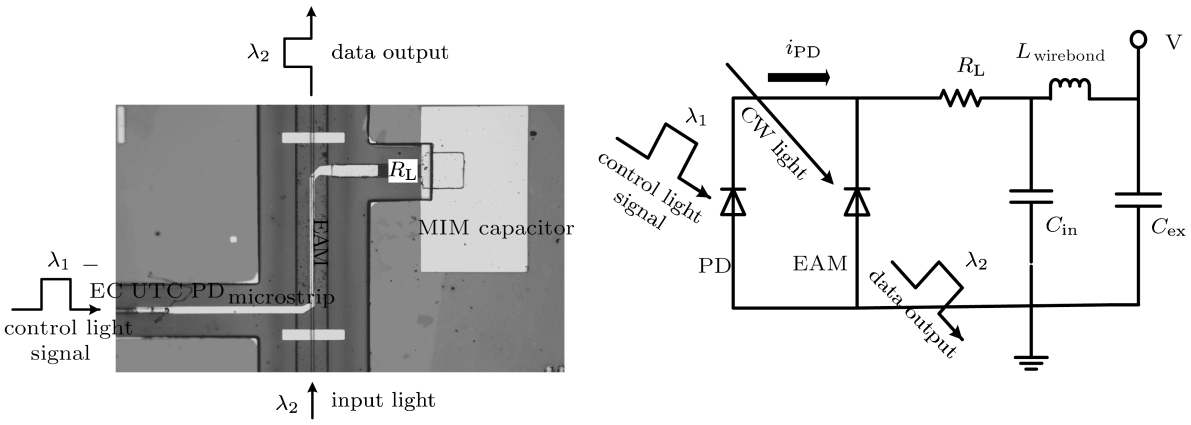


Fig. 1. (a) Chip photograph and (b) simplified circuit diagram of the monolithic EC-UTC-PD/EAM optical gate.

The epitaxial layer design of this optical gate is shown in Table 1. The EC-UTC-PD and the IQW-EAM share a common diluted waveguide. The IQW of EAM consists of ten periods of 1.57Q (which means a quaternary alloy with a bandgap of 1.57 microns wavelength)-InGaAsP wells (8 nm thick, 0.4% tensile strain), 1.4Q-InGaAsP barriers 6 nm thick, no strain) and 1.2Q-InGaAsP barriers (8-nm thick, 0.3% compressive strain). The overall tensile strain of IQW was used for the polarization independence. As shown in Table.1, the overall thickness of the IQW-EAM is similar to that of the EC-UTC-PD to ensure that the ridge waveguides can be formed simultaneously. The ridge waveguide of the IQW-EAM is 3 μm wide to provide single transverse-mode waveguide operation and has a 185 μm-long active part. The EC-UTC-PD ridge waveguide is 5 μm wide and has a 50 μm-long active part and a 20 μm-long passive coupled window.

Table 1. Epitaxial layer design of the EC-UTCPD/EAM optical gate.

epitaxial layer design of the IQW-EAM				epitaxial layer design of the EC-UTC-PD		
	material and thickness	doping/cm^{-3}			material and thickness	doping/cm^{-3}
17	200 nm InGaAs	P-Zn,1.0×10^{19}		17	150 nm InGaAs	P-Zn,1.0×10^{19}
16	1600 nm InP	P-Zn,1–10×10^{17}		16	500 nm P-InP	P-Zn,1×10^{18}
15	30 nm InP	u.i.d		15	200 nm 1.57Q	P-Zn,1–10×10^{17}cm^{-3}
14	100 nm 1.2Q	u.i.d		14	8 nm InP	u.i.d
13	8 nm 1.2Q(0.4%)	u.i.d		13	300 nm 1.4Q	u.i.d
12	6 nm 1.4Q	u.i.d	×10	12	150 nm 1.2Q	u.i.d
11	8 nm 1.56Q(-0.3%)	u.i.d		11	150 nm 1.2Q	1.0×10^{18}
10	80 nm 1.2Q	u.i.d		10	50 nm InP	1.0×10^{18}
9	150 nm InP	n-Si,1.0×10^{18}, the diluted waveguide layer				
8	60 nm 1.2Q	n-Si,1.0×10^{18}, the diluted waveguide layer				
7	200 nm InP	n-Si,1.0×10^{18}, the diluted waveguide layer				
6	60 nm 1.2Q	n-Si,1.0×10^{18}, the diluted waveguide layer				
5	250 nm InP	n-Si,1.0×10^{18}, the diluted waveguide layer				
4	60 nm 1.2Q	n-Si,1.0×10^{18}, the diluted waveguide layer				
3	300 nm InP	n-Si,1.0×10^{18}, the diluted waveguide layer				
2	60 nm 1.2Q	n-Si,1.0×10^{18}, the diluted waveguide layer				
1	50 nm InP	n-Si,1.0×10^{18}, the buffer layer				
0	(substrate)N-InP	S				

This optical gate is fabricated by a conventional two-step MOCVD growth and processing technique. For the first MOCVD growth, the buffer layer, the diluted waveguide layers, and the epitaxial layers of the superstructure of IQW-EAM are grown on an n-InP substrate. After the sample is patterned with SiO_2, the epitaxial layers of the superstructure of the IQW-EAM are removed by using selective chemical wet etching, with SiO_2 pattern used as mask. An MOCVD regrowth of the epitaxial layers of the superstructure of the UTC-PD is performed. The waveguides of EC-UTC-PD and IQW-EAM are determined by using reactive ion etching (RIE) simultaneously and the RIE dry etch stops within InP layer #9. To provide electrical isolation of passive part of the IQW-EAM, InGaAs contact layer is removed and a proton implantation is performed in this area. The passive coupled window of EC-UTCPD is determined by selective chemical wet etching of P-InGaAs, p-InP and p-1.57Q layers. After that, a 300 nm-thick SiN_x layer is deposited to capsulate the PD and the EAM, and it also serves as the dielectric film of the capacitor. A 2.5 μm-thick layer of photo-benzocyclobutene (BCB) is patterned and then p-metal is deposited. After the Ta_2N thin-film resistor is sputtered and patterned on the top of BCB layer, the wafer is thinned and back-side ohmic contact is formed via the evaporation of Au/Ge/Ni. The fabrication process is as simple as the process of making a single n-InP based EAM except for an additional MOCVD growth.

3. Test and device performances

The measured responsivity of EC-UTC-PD is over 0.6 A/W. The extinction ratio of the IQW-EAM versus reverse bias voltage for transverse electric (TE) polarized light with a wavelength of 1560 nm is shown in Fig. 2. With a power level of 10 mW, the sharp modulation efficiency of the IQW-EAM occurs at around −4 V. When the bias voltage is set at −4 V with a

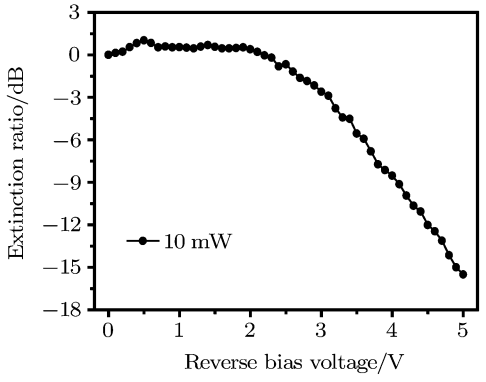


Fig. 2. Extinction ratio of the IQW-EAM versus reverse bias voltage for transverse electric (TE) polarized light with a wavelength of 156 nm.

control power of 12 mW incident into the EC-UTC-PD, the extinction ratio of the IQW-EAM is more than 15 dB.

The capacitances of on-chip bias capacitor $C_{\rm in}$, the IQW-EAM and the EC-UTC-PD are about 5 pF, 230 fF and 30 fF, respectively. The on-chip Ta_2N thin-film resistor is measured to be about 450 Ω. From expression (1), the device nominally has a 3 dB electrical switching bandwidth of 2.2 GHz. The bandwidth and the RF-gain were tested by a spectrum analyzer. Figure 3 shows the experiment setup used to measure the optical bandwidth of the optical gates. There are two optical inputs to the optical gates, one is a continuous wave light from a tunable laser at λ_2 incident into the modulator, and the other one is a swept frequency optical sinusoid signal at λ_1 generated by a Mach–Zehnder modulator incident into the EC-UTC-PD. The swept frequency signal at λ_2 output from the EAM is received by spectrum analyzer. There is only one electrical input for both EC-UTC-PD and EAM biases. Two erbium-doped fibre amplifiers (EDFAs) were used to amplify the optical signals, and an attenuator (ATTN) combined with a fibre power meter could be used to accurately set the power of the optical beam. $P_{\rm RF-in}(f)$ and $P_{\rm RF-out}(f)$ are frequency responses of signals coupled into the EC-UTC-PD and output from the IQW-EAM respectively. So optical amplitude response of the PD–EAM can be derived simply to be

$$|G(f)| = |P_{\rm RF-out}(f)/P_{\rm RF-in}(f)|. \qquad (2)$$

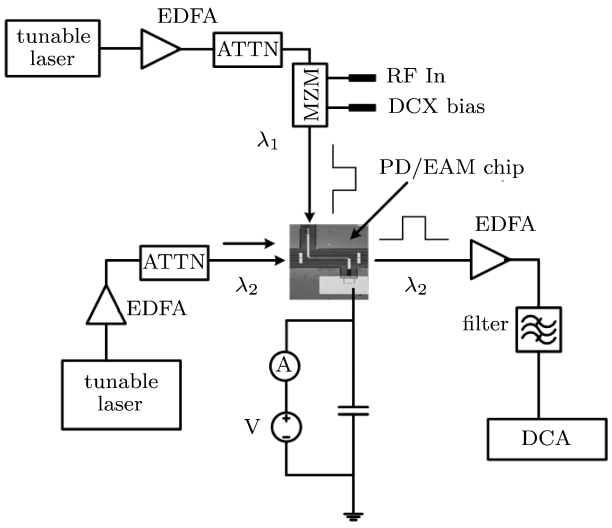


Fig. 3. Experimental setup for testing the optical bandwidth of the optical gates.

In this measurement, $P_{\rm RF-in}(f)$ and $P_{\rm RF-out}(f)$ were easily obtained by using a spectrum analyzer. The response of Mach–Zehnder modulator is flat bellow 2.5 GHz, so its influence can be neglected. Figure 4 shows the measured optical switching amplitude response of the PD–EAM optical gate derived from expression (2). The measurement was carried out at a continuous wave light wavelength of 1565 nm, and a control light of 1550 nm, an average photocurrent of 3.2 mA and a voltage bias of −3.7 V. The device in Fig. 4 exhibits 3 dB optical bandwidth of 2.1 GHz. A little discrepancy with the theoretical result is due mainly to the microwave propagation loss. Figure 5 shows the low frequency RF gain and the optical switching bandwidth of the PD–EAM optical gate against reverse bias voltage. It is shown that the RF gain first increases with reverse bias increasing until it comes to a maximum value of −13.2 dB at −4 V, and then decreases, while the 3 dB optical switching bandwidth increases with reverse bias increasing. The increase of the 3 dB optical switching bandwidth is attributed mainly to a reduction in the junction capacitances of EC-UTC-PD and IQW-EAM. The dependence of the RF gain on voltage is due mainly to the modulation slope efficiency of the EAM transfer curve and the maximum RF gain is about −16.2 dB at 2.1 GHz.

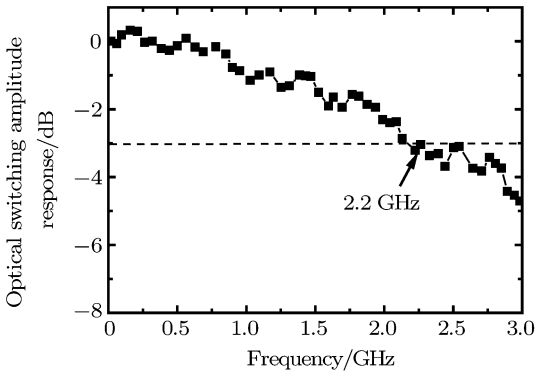


Fig. 4. Optical switching amplitude response of the PD–EAM measured by a spectrum analyzer.

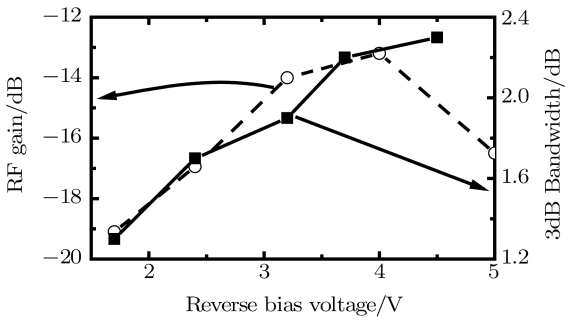


Fig. 5. Low frequency RF gain and optical switching bandwidth of the PD–EAM optical gate against the reverse bias voltage.

4. Conclusion

A novel PD–EAM optical gate, integrating a EC-UTC-PD with an IQWEAM, is fabricated on an n-InP substrate. With a 450 Ω load resistor, the bandwidth is about 2.1 GHz and a −16.2 dB RF-gain at 2.1 GHz is obtained. Even though the measured bandwidth is relatively low, we believe that, with further reducing the on-chip. Ta_2N thin-film resistor to 30 Ω, the EC-UTC-PD/EAM optical gate can be treated as a traveling wave structure and its bandwidth will be released from RC limitation.

Acknowledgement

The authors would like to thank Wang Bao-Jun, Zhou Fan, and Shu Hui-Yun for their help in the experiment, and also Wang Lu-Feng, Bian Jing and An Xin for the device test.

References

[1] Yoo S J B 1996 *IEEE J. Light. Tech.* **14** 995
[2] Sabnis V A, Demir H V, Fidaner O, Harris J S, Miller D A B, Zheng J F, Li N, Wu T C, Chen H T and Houng Y M 2004 *Appl. Phys. Lett.* **84** 469
[3] Xu X J, Chen S W, Xu H H, Sun Y, Yu Y D, Yu J X and Wang Q M 2009 *Chin. Phys.* B **18** 3900
[4] Wang J, Sun J and Zhang X 2008 *Electronic Letters* **44** 413
[5] Kodama S, Yoshimatsu T and Ito H 2004 *Electron. Lett.* **40** 555
[6] Yoshimatsu T, Kodama S, Yoshino K and Ito H 2004 *Electron. Lett.* **40** 626
[7] Kodama S, Shimizu T, Yoshimatsu T, Yoshino K, Furuta T and Ito H 2004 *Electron. Lett.* **40** 696
[8] Yoshimatsu T, Kodama S, Yoshino K and Ito H 2005 *IEEE Photon. Technol. Lett.* **17** 2367
[9] Zhang Y X, Liao Z Y, Pan J Q, Zhou F, Zhu H L, Zhao L J and Wang W 2009 *Chin. Phys. Lett.* **26** 034215-1
[10] Yoshino K, Yoshimatsu T, Kodama S and Ito H 2006 *IEEE Trans. Adv. Packag.* **29** 766
[11] Achouche M, Magnin V, Harari J, Lelarge F, Derouin E, Jany C, Carpentier D, Blache F and Descoster D 2004 *IEEE Photon. Technol. Lett.* **16** 584
[12] Zhang Y X, Pan J Q, Zhao L J, Zhu H L and Wang W 2010 *Chin. Phys. Lett.* **27** 028501
[13] Shin D S and Yu P K L 2001 *J. Appl. Phys.* **89** 1515
[14] Chen J X, Wu Y, Chen W X, Shubin I, Clawson A, Chang W S C and Yu P K L 2004 *IEEE Photon. Technol. Lett.* **16** 440
[15] Zhang Y X, Liao Z Y and Wang W 2009 *Chin. Phys.* B **18** 2393
[16] Demir H V, Sabnis V A, Fidaner O, Zheng J, Harris J S and Miller D A B 2005 *IEEE J. Sel. Topics Quantum Electron.* **11** 86